ISBN: 978-3-95450-229-5 ISSN: 2673-5520 doi:10.18429/JACoW-MEDSI2020-TUOB02

DEVELOPMENT OF A PASSIVE TUNED MASS DAMPER FOR ULTRA-HIGH VACUUM BEAMLINE OPTICS

F. Khan, D. Crivelli, J. Kelly, A. Male, Diamond Light Source Ltd., Didcot, England

Abstract

Vibration in beamline optics can degrade the quality of experiments: the resulting movement of a mirror increases the X-ray beam position uncertainty and introduces flux variations at the sample. This is normally dealt with by averaging data collection over longer periods of time, by slowing down the data acquisition rates, or by accepting low-quality blurred images. With the development of faster camera technology and smaller beam sizes in next generation synchrotron upgrades, older optics designs can become less suitable, but still very expensive to redesign.

Mechanically, mirror actuation systems require a balance between repeatability of motion and stability. This leads to designs that are "soft" with resonant modes at a relatively low frequency, which can be easily excited by external disturbances such as ground vibration and local noise. In ultra-high vacuum applications, the damping is inherently low, and the vibration amplification at resonance tends to be very high.

At Diamond we designed a process for passively damping beamline mirror optics. First, we experimentally analyse the mirror's vibration modes; we then determine the tuned mass damper (TMD) parameters using mathematical and dynamic models. Finally, we design a flexure-based metal TMD which relies on eddy current damping through magnets and a conductor plate. The TMD can be retrofitted using a clamping system that requires no modification to the existing optic. In this conference paper we show a case study on a mirror system on Diamond Light Source's Small Molecule Single Crystal Diffraction Beamline, I19.

INTRODUCTION

The vibrational behaviour of the Horizontally Focusing Mirror (HFM) at I19 (Fig. 1) was evaluated upon witnessing low resonant signatures in the Fast Fourier Transform (FFT) of the X-ray beam positioning data. Figure 2 shows

Figure 1: The HFM sitting on actuators is placed at the Small Molecule Single Crystal Diffraction Beamline, I19, at Diamond Light Source.

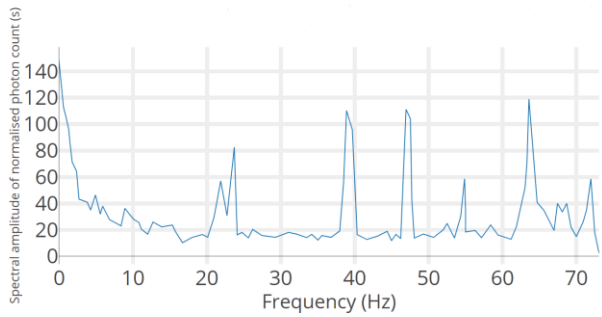

Figure 2: FFT plot of the HFM X-ray beam stability.

distinct peaks at 23, 40 and 47 Hz respectively. An experimental modal analysis characterised these natural frequencies with rocking and pitching modes in the actuators, which would magnify with distance from the centre of the mirror and affect beam positioning if left untreated.

A proposition was developed to house four retrofitted tuned mass dampers (TMDs) to effectively dampen the specific resonances. The TMDs would be installed and secured using slide-in trays and clamps, virtually leaving the expensive mirror system unchanged.

3D PRINTED TMD

An initial 3D printed TMD prototype was tuned to target the 23 Hz mode, as shown in Fig. 3. The monolithic design used calibrated double-hinged PLA flexures [1] (shown in purple) as a means of lateral motion and dissipation of energy through eddy current damping (ECD) (permanent magnets shown in yellow). The derived theory behind the flexure geometry is discussed under Design Process.

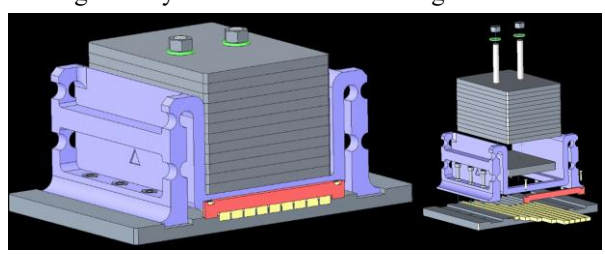

Figure 3: A representation of the 3D printed monolithic TMD prototype in a CAD assembly.

The passive vibration of the HFM was experimentally measured once more with the mounted TMD prototype. In the FFT plot (Fig. 4), the amplitude of the 23 Hz resonance visibly decreased with no additional parasitic motion introduced to the system. The 15 Hz peak, found to be a translation mode, was present during vibrational testing but was not registered by the beam positioning data seen in Fig. 2, hence it was disregarded.

ISBN: 978-3-95450-229-5 ISSN: 2673-5520 doi:10.18429/JACoW-MEDSI2020-TUOB02

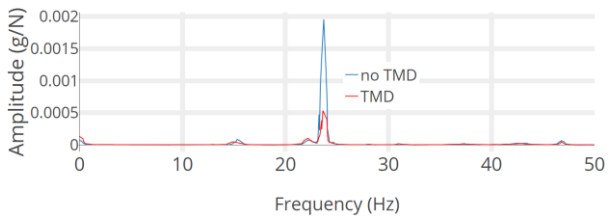

Figure 4: FFT plot showing a reduction in amplitude at 23.75 Hz in the presence of the TMD (red), measured using an accelerometer mounted on the optic.

Fundamentally, a TMD's effectiveness is controlled by material tolerances and manufacturing capabilities. Whilst 3D printing is recognised as the optimal solution for complex geometries, fabricating a printed flexure from ULTEM [2] revealed higher risk with little additional cost benefit. Most additive manufacturing operations, particularly using ULTEM, still experience limitations in repeatability and precision [3]. Although ULTEM is vacuum compatible, its performance and durability would require additional testing; dedicating time for such an inspection would have imposed extra delays on the beamline. Consequently, conventionally machined metallic flexures were opted as a reliable alternative which required a total redesign of the TMD.

DESIGN PROCESS

The redesign focussed on four key principles: compatibility with the ultra-high vacuum (UHV) environment, configurability, machinability, and precision. First the mass, stiffness and damping requirements were determined [4] (Table 1). The mass, limited to 4kg per TMD, was defined by the maximum weight the housing could support without compromising the mirror's performance.

Next the geometry of the flexure was configured to achieve the target stiffness, k2. Equation 1 was derived from first principles through likening the double-hinge stiffness to torsional springs [5] (Fig. 5).

$$k_{2\_flexure} = \frac{16Ebt^{\frac{5}{2}}}{9\pi {L_2}^2 R^{\frac{1}{2}}} \qquad (1)$$

The final model for the TMD is shown in Fig. 6. The values for b, t, R, and L_2 were chosen with spatial limitations in mind (Fig. 6a). Table 2 summarises the main design features and how they satisfy the four principles mentioned earlier.

Table 1: Initial Parameters and Equations [4]

Parameter	Symbol	Equation	Units
Inertial Moment	J	From CAD Model	kgm^2
Inertial Radius	R	From CAD Model	m^2
Modal mass	m_1	$(Jr^2)/2$	kg
Frequency	f_1	Chosen	Hz
TMD Target			
Mass	m_2	Chosen	kg
Mass ratio	μ	m_2/m_1	-
Frequency	f_2	$(1/(1+\mu))f_1$	Hz
Stiffness	k_2	$(2\pi f_2)^2 m_2$	N/m
Relative damping	ξ	$\sqrt{3\mu/(8(1+\mu))}$	-
Absolute damping	c_2	$2\xi\sqrt{k_2 m_2}$	Ns/m

DESIGN ANALYSIS

Simscape

Before procurement and prototype testing, the suitability of the design was explored through simulations [7] and creating dynamic models [8]. A double-mass-spring system was set-up in MATLAB and Simscape using the initial inputs found from Table 1. The quick solving time allowed for "what-if" scenario iterations, hence establishing a desired tolerance for the flexure geometry which could be communicated to the manufacturers.

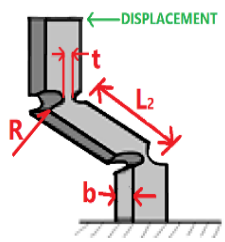

Figure 5: Dimensions of one double-hinge flexure column that support Eq. 1, with E = Young's Modulus

Table 2: Main Design Attributes

	UHV	Configurability	Machinability	Precision
Flexures	Aluminium 6082-T6	Flexures can be swapped out.	Simultaneously cut two flexures per TMD to form matched pair.	Wire-EDM achieves 20-micron tolerance [6].
Mass	Stainless steel 304L	More/less mass plates can be suspended.	-	Smaller mass plates used for fine-tuning.
ECD	Can survive baking and cleaning prior to UHV insertion.	Adjustable distance between conductor/magnets. Magnets can be changed.	No viscoelastics.	Prototype testing determines optimal damping arrangement.

ISBN: 978-3-95450-229-5 ISSN: 2673-5520 doi:10.18429/JACoW-MEDSI2020-TUOB02

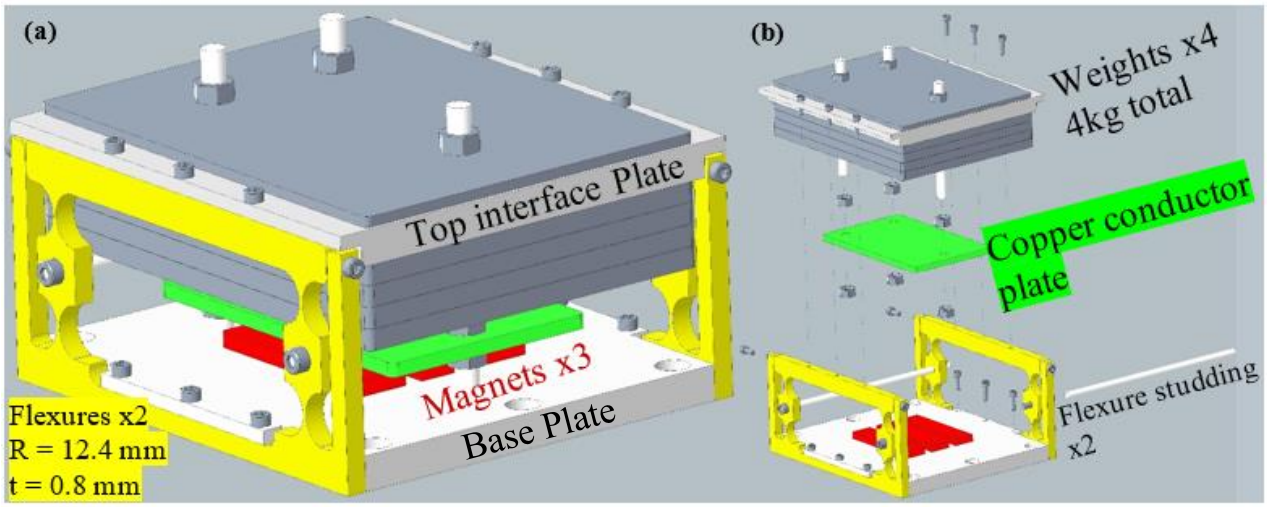

Figure 6: (a) A final CAD representation of the 23 Hz machined TMD prototype with annotations; (b) Exploded view showing how the mass component can be completely detached and reassembled with ease.

ANSYS

A buckling and stress analysis confirmed that the flexure would remain below yield stress when subjected to less than 0.4mm displacement during operation. A harmonic analysis predicted the natural frequency behaviour of the TMD. Any modes present after the expected resonance were critically required to be >100 Hz to prevent parasitic motion interfering with the HFM in operation. The ANSYS solution revealed a translational mode in the off-axis of the TMD at ~80Hz. Steel studding between the flexure pair (Fig. 6b) helped to increase this lateral stiffness, which seemed to be enough to shift the second mode above 80 Hz in the simulation.

PROTOTYPE TESTING

In-house experimental testing verified the modal behaviour of the machined TMD prototype in comparison to the ANSYS simulation. Simultaneously, the optimal ECD conditions were met by testing a combination of different strength magnets and polarity arrangements.

The time-based plot (Fig. 7a) shows a steep decay in oscillations with a damping ratio of 3.16%. The FFT plot (Fig. 7b) consistently displayed a sharp resonance at 15.5 Hz between repeats, but also an auxiliary peak at ~40-50 Hz. Hence, the TMD was performing as expected, but the real off-axis stiffness was at a resonance much lower than ANSYS predicted. This highlighted two design changes: (1) Accommodate up to 6 strong magnets to achieve higher damping, and (2) Machine a stainless-steel spacer block to replace the flexural studding and increase lateral stiffness further.

The final comparison between all the models can be summarised in Table 3. The prototype performed within +-0.5Hz of the target frequency with an error of 2.82%

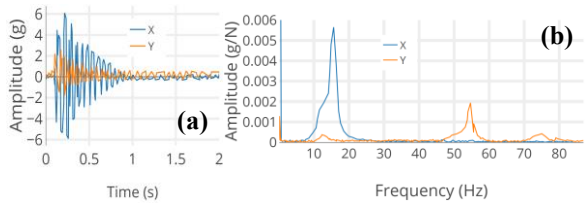

Figure 7: (a) Time-based plot showing a steep decay in oscillations during ECD; (b) FFT plot showing a distinct peak at 15.5Hz in the desired x-direction, and an orthogonal peak at 54 Hz in the y-direction as measured by an accelerometer.

Table 3: Model Parameter Value Comparison

	TARGET	Theory	ANSYS	Prototype
f_2 [Hz]	15.9	16.2	16.3	15.5
k_2 [N/m]	40202	40204	41755	36715
m_2 [kg]	4.00	3.94	3.99	3.87

CONCLUSION

This report outlined the justification and process behind designing and retrofitting machined TMDs to remove undesirable motion of the HFM in I19. Once the mirror is open for installation later in the year, all four TMDs will be fitted and tuned; the optic stability will be remeasured with an accelerometer and validated with X-ray data. This in-house design procedure utilises the best engineering practises whilst emphasising the importance of conscientious modelling before procurement, which will lead to optimised damping designs that will work first time. The end-product is entirely passive and undisruptive, which will allow beamline users to continue invaluable research at the facility.

ISBN: 978-3-95450-229-5 ISSN: 2673-5520 doi:10.18429/JACoW-MEDSI2020-TUOB02

REFERENCES

[1] A. H. Slocum, "Precision Machine Design," United States, Society of Manufacturing Engineers, 1993, Topic 17, pp. 1-20.

[2] StrataSys, "ULTEM™ 1010 Resin Data Sheet," https://info.stratasysdirect.com/rs/626-SBR-192/images/Data%20Sheet%20-%20%20EN%20ULTEM%201010.pdf

[3] Formlabs, "Understanding Accuracy, Precision, and Tolerance in 3D Printing," https://formlabs.com/blog/understanding-accuracy-precision-tolerance-in-3d-printing

[4] J. Vink, "Flexure hinges: theory and practice," Vink System Design & Analysis, https://www.vinksda.com/flexure-hinges-theory-and-practice/?web=1&wdLOR=cF383EDB8-0AEF-45A7-83C0-0735E2E062BE

[5] J. Paros and L. Weisbord, "How to design flexure hinges," *Machine Design,* vol. 37, pp. 151–156, 1965.

[6] "Electrical discharge machining," Wikipedia, The Free Encyclopedia, https://en.wikipedia.org/w/index.php?title=Electrical_discharge_machining&oldid=1029272834

[7] I. Hussain *et al.*, "Multi-Physical Design and Resonant Controller Based Trajectory Tracking of the Electromagnetically Driven Fast Tool Servo," *Actuators,* vol. 9, no. 2, p. 28, 2020. https://doi.org/10.3390/act9020028h

[8] X. Chen, "Optimization and estimation routine for tuned mass damper," Blekinge Institute of Technology, Karlskrona, Sweden, 2010.